Ezh2 is required for neural crest-derived cartilage and bone formation

Schwarz, Daniel ; Varum, Sandra ; Zemke, Martina ; Schöler, Anne ; Baggiolini, Arianna ; Draganova, Kalina ; Koseki, Haruhiko ; Schübeler, Dirk ; Sommer, Lukas

Abstract: The emergence of craniofacial skeletal elements, and of the jaw in particular, was a crucial step in the evolution of higher vertebrates. Most facial bones and cartilage are generated during embryonic development by cranial neural crest cells, while an osteochondrogenic fate is suppressed in more posterior neural crest cells. Key players in this process are Hox genes, which suppress osteochondrogenesis in posterior neural crest derivatives. How this specific pattern of osteochondrogenic competence is achieved remains to be elucidated. Here we demonstrate that Hox gene expression and osteochondrogenesis are controlled by epigenetic mechanisms. Ezh2, which is a component of polycomb repressive complex 2 (PRC2), catalyzes trimethylation of lysine 27 in histone 3 (H3K27me3), thereby functioning as transcriptional repressor of target genes. Conditional inactivation of Ezh2 does not interfere with localization of neural crest cells to their target structures, neural development, cell cycle progression or cell survival. However, loss of Ezh2 results in massive derepression of Hox genes in neural crest cells that are usually devoid of Hox gene expression. Accordingly, craniofacial bone and cartilage formation is fully prevented in Ezh2 conditional knockout mice. Our data indicate that craniofacial skeleton formation in higher vertebrates is crucially dependent on epigenetic regulation that keeps in check inhibitors of an osteochondrogenic differentiation program.

DOI: https://doi.org/10.1242/dev.094342

© 2014. Published by The Company of Biologists Ltd | Development (2014) 141, 867-877 doi:10.1242/dev.094342

RESEARCH ARTICLE

Ezh2 is required for neural crest-derived cartilage and bone formation

Daniel Schwarz[1,‡], Sandra Varum[1,‡], Martina Zemke[1], Anne Schöler[2,*], Arianna Baggiolini[1], Kalina Draganova[1], Haruhiko Koseki[3], Dirk Schübeler[2,4] and Lukas Sommer[1,§]

ABSTRACT

The emergence of craniofacial skeletal elements, and of the jaw in particular, was a crucial step in the evolution of higher vertebrates. Most facial bones and cartilage are generated during embryonic development by cranial neural crest cells, while an osteochondrogenic fate is suppressed in more posterior neural crest cells. Key players in this process are Hox genes, which suppress osteochondrogenesis in posterior neural crest derivatives. How this specific pattern of osteochondrogenic competence is achieved remains to be elucidated. Here we demonstrate that Hox gene expression and osteochondrogenesis are controlled by epigenetic mechanisms. Ezh2, which is a component of polycomb repressive complex 2 (PRC2), catalyzes trimethylation of lysine 27 in histone 3 (H3K27me3), thereby functioning as transcriptional repressor of target genes. Conditional inactivation of *Ezh2* does not interfere with localization of neural crest cells to their target structures, neural development, cell cycle progression or cell survival. However, loss of Ezh2 results in massive derepression of Hox genes in neural crest cells that are usually devoid of Hox gene expression. Accordingly, craniofacial bone and cartilage formation is fully prevented in *Ezh2* conditional knockout mice. Our data indicate that craniofacial skeleton formation in higher vertebrates is crucially dependent on epigenetic regulation that keeps in check inhibitors of an osteochondrogenic differentiation program.

KEY WORDS: Ezh2, Epigenetic regulation, Neural crest, Chondrogenesis, Osteogenesis, Mouse

INTRODUCTION

Neural crest cells (NCCs) are a transient, multipotent population of cells that are specified during embryonic development in the neural tube and then delaminate from the dorsal tip during closure of the neural tube. NCCs give rise to a variety of neural and non-neural cell types (Gammill and Bronner-Fraser, 2003). Depending on the level of emigration along the rostral-caudal axis of the embryo, the NC can be divided into distinct subpopulations that differ in the cell fates that they generate. Trunk NCCs build up a large part of the peripheral nervous system (PNS), including Schwann cells of peripheral nerves and neurons and glia of sympathetic, parasympathetic and sensory ganglia (Le Douarin and Dupin, 2012). In addition, they give rise to melanocytes (Sommer, 2011) and endocrine cells (Le Douarin and Dupin, 2012). Cranial neural crest cells (CNCCs) emigrate from the caudal forebrain, midbrain and hindbrain to the level of the first somite and give rise to additional cell fates in comparison to trunk NCCs, contributing to cartilage, bone and connective tissue (Le Douarin et al., 2007; Santagati and Rijli, 2003). CNCCs migrate into the branchial arches (BAs), becoming NC-derived mesenchymal progenitor cells (MPCs), which produce cartilage and skeletogenic elements of the craniofacial region. Specific cell fates of CNCCs are controlled by positional cues that determine intrinsic gene expression patterns that are partially specified already at emigration from the neural tube. Central players in this process are the Hox genes that are differentially expressed in migratory CNCCs and BAs according to the axial position. In particular, cells in BA1 and anterior domains are devoid of Hox gene expression, which allows formation of the chondrogenic and skeletal elements of the facial region (Creuzet et al., 2002; Kanzler et al., 1998; Minoux and Rijli, 2010). In addition to these intrinsic cues, CNCC fates are regulated by environmental signals, such as Tgfβ (Wurdak et al., 2006) and Fgf8 expressed from the facial and BA ectoderm (Le Douarin et al., 2007; Santagati and Rijli, 2003). As a consequence of such signaling, expression of the transcription factor Sox9 is upregulated in MPCs, while expression levels of the NC specifier gene and NC stem cell (NCSC) marker Sox10 decrease (John et al., 2011). This switch in Sox transcription factor expression leads to suppression of neural fates and allows CNCCs to differentiate into mesectodermal NC derivatives, including bone, cartilage and smooth muscle.

Polycomb repressive complex 2 (PRC2) is composed of four core subunits: enhancer of zeste homolog 2 (Ezh2), embryonic ectoderm development (Eed), suppressor of zeste 12 (Suz12) and RbAp46/48 (Rbbp4/7 in mouse) (Margueron and Reinberg, 2011). Ezh2, with its SET domain, is the catalytic subunit of PRC2 that catalyzes the mono-, di- and trimethylation of H3K27 (H3K27me1, H3K27me2 and H3K27me3) (Shen et al., 2008). PRC2 modulates gene expression via H3K27 trimethylation and acts as a transcriptional repressor (Mikkelsen et al., 2007; Schuettengruber et al., 2007). In mammals, PRC2 is involved in repressing developmental regulators in mouse embryonic stem cells (mESCs) and in regulating the proliferation and differentiation of stem cells (Boyer et al., 2006; Margueron and Reinberg, 2011). The importance of epigenetic modifiers in vertebrate development is evident from the phenotype of mice lacking *Ezh2*, which die around gastrulation (O'Carroll et al., 2001). Later in development, the need for epigenetic modifiers is stage and time dependent and also functionally distinct from that in ESCs. For example, neural stem cells that lack *Ezh2* exhibit a prolonged neurogenic phase even though differentiation is not affected (Hirabayashi et al., 2009). Other experiments have shown a role for *Ezh2* in regulating anterior-posterior axis specification and proximo-distal axis elongation in the developing limb bud

[1]Cell and Developmental Biology, Institute of Anatomy, University of Zurich, CH-8057 Zurich, Switzerland. [2]Friedrich Miescher Institute for Biomedical Research, CH 4058 Basel, Switzerland. [3]RIKEN Center for Integrative Medical Sciences, Yokohama City, Kanagawa 230-0045, Japan. [4]University of Basel, Faculty of Sciences, 4051 Basel, Switzerland.
*Present address: Helmholtz Zentrum, 85764 Neuherberg, Germany.
‡These authors contributed equally to this work

§Author for correspondence (lukas.sommer@anatom.uzh.ch)

Received 18 January 2013; Accepted 20 November 2013

Development (2014) doi:10.1242/dev.094342

(Wyngaarden et al., 2011). Furthermore, Soshnikova and Duboule demonstrated H3K27me3 occupancy over the HoxD gene cluster in the developing tail bud of mice, which points to direct regulation of developmental regulators by epigenetic modifications and, more specifically, an involvement of Ezh2 (Soshnikova and Duboule, 2009). Evidence for a direct regulation of NCCs by epigenetic modifiers comes from the work of Strobl-Mazzulla and colleagues, who showed direct regulation of *Sox10* by the histone demethylase Jmjd2a (Kdm4a in mouse) (Strobl-Mazzulla et al., 2010).

These findings suggest that the regulation of NCC specification, migration, proliferation and differentiation is at least partially dependent on epigenetic regulators and modifiers, although the specific factors and modifications directly involved in the epigenetic regulation of NC development remain to be determined. In the present study, we examined the role of *Ezh2* in NC development by conditionally ablating *Ezh2* in premigratory NCCs *in vivo*. Surprisingly, loss of Ezh2-mediated H3K27 trimethylation had no overt effect on NCC migration and PNS formation. Likewise, establishment of MPCs in BAs and the cell cycle properties of MPCs were not impaired. By contrast, NC-derived craniofacial structures failed to form from MPCs, which was accompanied by derepression of Hox genes in CNCCs lacking *Ezh2*. This phenotype demonstrates a highly specific role of *Ezh2* in NCC subpopulations and points to a crucial involvement of epigenetic control mechanisms in the development of jawed vertebrates.

RESULTS

Inactivation of *Ezh2* in NCCs

In order to address the *in vivo* role of *Ezh2* during NC development, we mated mice homozygous for the floxed allele of *Ezh2* (Hirabayashi et al., 2009) with mice heterozygous for the floxed allele that additionally carried a transgene expressing Cre recombinase under the *Wnt1* promoter (Danielian et al., 1998) (supplementary material Fig. S1A). *Ezh2* conditional knockout (cko) mice survived to late developmental stages, but were never born. To determine the loss of *Ezh2* transcripts, we performed quantitative RT-PCR of mRNA isolated from BA1 cells. We used two different primer sets, one targeting *Ezh2* exons 18 and 19 and the other exons 5 to 8 (Ezh2 E18-19 and Ezh2 E5-8). The Ezh2 E18-19 primers recognize sequences in the mRNA transcript that encode part of the SET domain, whereas the Ezh2 E5-8 primer set targets a sequence 5′ to the SET domain. Both quantitative RT-PCR reactions showed a comparable and significant reduction of the *Ezh2* mRNA transcript in *Ezh2* cko embryos compared with controls (supplementary material Fig. S1B).

To track the fate of NCCs lacking *Ezh2* upon Cre-mediated gene deletion, we used the *ROSA26* Cre reporter allele (*R26R*) (Soriano, 1999). In mice carrying this allele, all NCCs express β-galactosidase due to *Wnt1*-Cre-dependent recombination (Chai et al., 2000; Hari et al., 2002). First, we examined changes in the main functional readout of Ezh2 activity by performing immunohistochemistry for H3K27me3. In the trunk of *Ezh2* cko embryos at embryonic day (E) 9.5, virtually all migratory NCCs identified by β-galactosidase expression lacked H3K27me3, in contrast to control embryos (Fig. 1A-C). Likewise, Ezh2-dependent H3K27me3 was lost in NCCs populating the BA1 of *Ezh2* cko embryos (Fig. 1D-F). Taken together, these results demonstrate efficient inactivation of *Ezh2* in NC-derived cells upon conditional knockout of *Ezh2* in NCCs.

Migration of NCCs and their localization to target structures are not impaired by loss of *Ezh2*

In vivo fate mapping of NCCs by means of the *ROSA26* Cre reporter allele did not reveal any differences between *Ezh2* cko and control

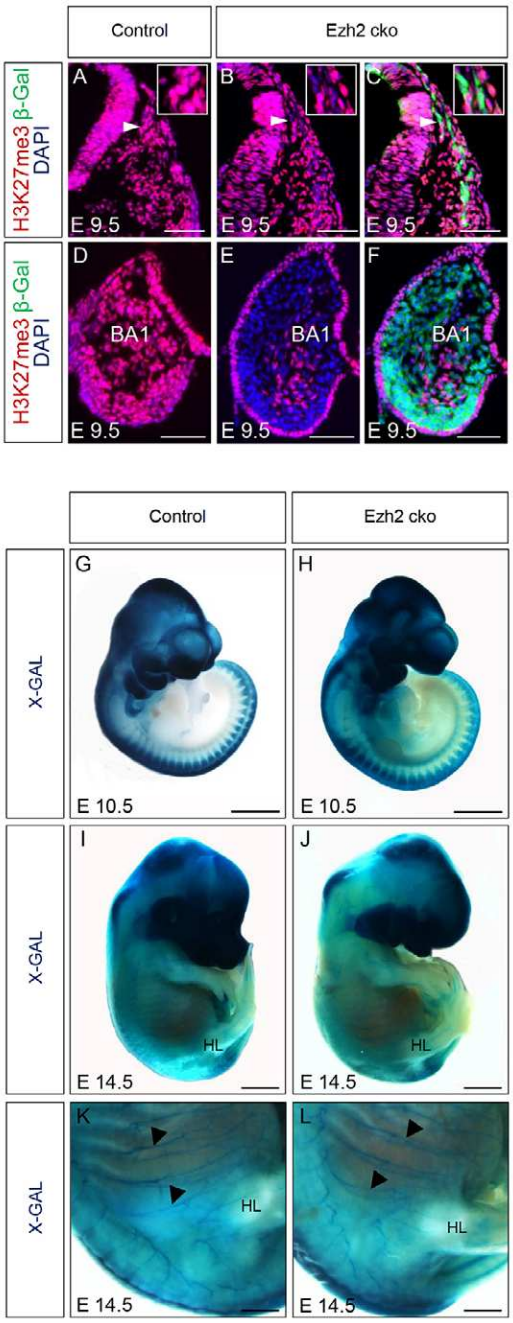

Fig. 1. Migration of NCCs to their target structures is not impaired by loss of *Ezh2*. (A-F) *Wnt1-Cre*-mediated ablation of *Ezh2* results in loss of H3K27me3 in mouse E9.5 neural crest stem cells (NCSCs). To detect NCSCs lacking *Ezh2* upon Cre-mediated recombination we used the *R26R* Cre reporter allele. In contrast to control NCSCs, both trunk (A-C) and BA1 (D-F) *Ezh2* mutant NCSCs lacked H3K27me3 by E9.5. Arrowheads indicate regions magnified in insets. (G,H) *In vivo* fate mapping of neural crest cells (NCCs) in E10.5 control and *Ezh2* cko embryos. NCCs expressing β-galactosidase were visualized by X-Gal whole-mount staining. Both genotypes show a comparable localization of NCCs to their supposed target structures. (I,J) *In vivo* fate mapping of NCCs in E14.5 embryos with the *R26R* Cre reporter allele, indicating a severe loss of almost all craniofacial derivatives of cranial neural crest cells (CNCCs). (K,L) Higher magnification of the caudal part of the E14.5 control and *Ezh2* cko embryos shown in I and J. Peripheral nerves are present in both genotypes (arrowheads), indicating normal development of peripheral nerves. BA, branchial arch. HL, hind limbs. Scale bars: 50 µm in A-F; 2 mm in G-J; 1 mm in K,L.

Development (2014) doi:10.1242/dev.094342

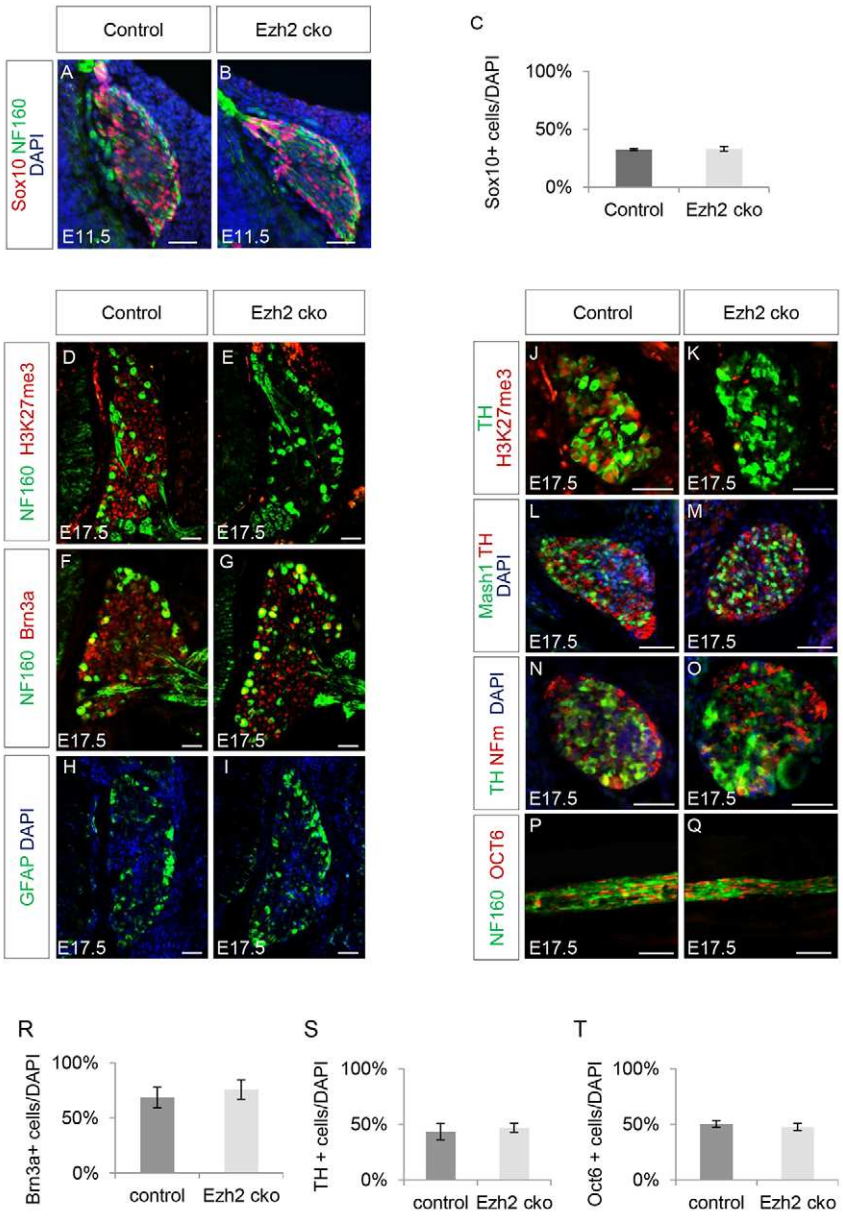

Fig. 2. Loss of H3K27me3 does not interfere with the differentiation of trunk NCCs. (A-C) Immunohistochemistry and quantification of Sox10^{+} cells indicates that conditional ablation of *Ezh2* in the NC does not hinder Sox10 expression in the forming dorsal root ganglia (DRG) of E11.5 *Ezh2* cko embryos. Loss of H3K27me3 is maintained during development of *Ezh2* cko embryos as shown by H3K27me3 immunohistochemistry for E17.5 DRG (D,E) and autonomic ganglia (AG) (J,K). Nonetheless, *Ezh2* cko and control embryos express similar levels of the late stage neuronal marker NF160 in the DRG (D-G), as well as similar levels of the dopaminergic neuronal marker TH in the AG (J-O,S). (F,G,R) Additionally, *Ezh2* cko DRG contain similar numbers of cells positive for the sensory progenitor marker Brn3a when compared with control DRGs. (H,I) The satellite glial marker Gfap was expressed in a similar fashion in control and *Ezh2* cko embryos. (L,M) Also, the autonomic progenitor marker Mash1 was found to be expressed similarly in control and *Ezh2* cko. (P,Q,T) Peripheral nerves, highlighted by NF160, of E17.5 control and *Ezh2* cko embryos express similar levels of the immature Schwann cell marker Oct6. Data are presented as mean percentage of positive cells/DAPI ± s.e.m. Scale bars: 50 µm.

embryos stained with X-Gal for β-galactosidase activity. NCCs lacking *Ezh2* migrated to and populated the structures normally built up by NCCs, such as the BAs and dorsal root ganglia (DRG) (Fig. 1G,H). At E11.5, it was still not possible to macroscopically distinguish *Ezh2* cko embryos from control embryos (data not shown). These results suggest that early events of NC specification and migration to the respective targets are not profoundly affected by the loss of *Ezh2* in NCCs.

However, *Ezh2* cko embryos displayed an overt, macroscopically detectable phenotype from E12.5 onwards, as illustrated by X-Gal staining of E14.5 embryos carrying the *R26R* allele (Fig. 1I,J). Whereas analysis at hindlimb levels pointed to normal development of peripheral nerves in *Ezh2* cko embryos (Fig. 1K,L, arrowheads), mutant embryos exhibited severe craniofacial malformations, despite the presence of residual β-galactosidase-expressing cells in the nasofrontal area (Fig. 1I,J). Thus, Ezh2 activity appears to be dispensable for proper localization of NCCs to target tissues and their long-term survival, but is required for the morphogenesis of particular NC derivatives.

Ezh2 is not required for neuronal and glial differentiation of NCCs

To assess the role of Ezh2 in trunk NCC differentiation we performed immunohistochemistry staining on transverse sections of *Ezh2* cko and control embryos at E11.5. Quantification revealed that the number of cells in the forming DRG expressing Sox10, a marker for NCSCs and the glial lineage, was unaltered upon conditional *Ezh2* ablation (Fig. 2A-C). Likewise, the neuronal marker neurofilament 160 (NF160; Nefm – Mouse Genome Informatics) was expressed normally in *Ezh2* cko embryos at this stage. In DRG at E17.5, absence of H3K27me3 confirmed the persistent loss of Ezh2 activity in *Ezh2* cko embryos compared with control littermates (Fig. 2D,E). Expression analysis of the sensory neuronal differentiation marker Brn3a (Pou4f1 – Mouse Genome Informatics) (Eng et al., 2004) and of NF160 did not reveal any differences between *Ezh2* cko and control embryos (Fig. 2F,G). Likewise, satellite cell formation and differentiation appeared to be normal in DRG lacking *Ezh2*. Indeed, immunohistochemistry for glial fibrillary acidic protein (Gfap), a

Development (2014) doi:10.1242/dev.094342

late marker of glial differentiation, and staining for fatty acid binding protein (FABP), an early marker of the glial lineage, did not reveal any alterations at E17.5 after *Ezh2* ablation in the NC (Fig. 2H,I; data not shown).

As in DRG, we found the expected loss of Ezh2-mediated histone methylation in autonomic ganglia (AG) of *Ezh2* cko embryos at E17.5 (Fig. 2J,K). However, Mash1 (Ascl1 – Mouse Genome Informatics), a progenitor marker for autonomic neurons, and tyrosine hydroxylase (TH), a marker for terminally differentiated autonomic neurons, were both present in AG of *Ezh2* cko embryos, as in control embryos (Fig. 2J-O). Similarly, Oct6 (Pou3f1 – Mouse Genome Informatics), a marker expressed in premature Schwann cells, was expressed in peripheral nerves of *Ezh2* cko mice in a manner comparable to control peripheral nerves. Mutant peripheral nerves also stained normally for NF160 (Fig. 2P,Q). Quantification of the immunohistochemical data confirmed that formation of the sensory, autonomic and glial lineages was not overtly affected by the loss of *Ezh2* (Fig. 2R-T). Our results indicate, therefore, that global loss of H3K27me3 in NCCs does not interfere with PNS differentiation steps.

Ezh2 depletion in NCCs causes severe craniofacial defects

Gross morphological analysis of *Ezh2* cko embryos pointed to a requirement of H3K27me3 for proper BA differentiation and morphogenesis of craniofacial structures (Fig. 1I,J). To further investigate this phenotype, we assessed cartilage and bone formation in *Ezh2* cko embryos at different developmental stages. As shown by Alcian Blue staining, conditional ablation of *Ezh2* in NCCs resulted in loss of all the chondrogenic structures that build up the skeletogenic elements of the craniofacial structures (Fig. 3A-D). At E14.5, *Ezh2* cko embryos lacked the upper and lower jaws as well as the nasofrontal plate (Fig. 3C,D). At E17.5, staining with both Alcian Blue and Alizarin Red (labeling bone) showed that almost all facial skeletal elements were absent in *Ezh2* cko embryos (Fig. 3E,F). Elements completely derived from CNCCs were absent, whereas skull bones, to which CNCCs are just beginning to contribute at this stage, appeared abnormal but were established (Gross and Hanken, 2008; Jiang et al., 2002). Parts of the parietal skeletal plate and the interparietal plate were detectable (Fig. 3E,F). Bones derived exclusively from CNCCs, such as the mandible, maxillary or the nasofrontal plate, were completely missing in *Ezh2* cko embryos at E17.5 (Fig. 3E,F). Chondrogenic elements, such as the otic capsule, were partially established in the back of the head (Fig. 3E,F), but, more rostrally, chondrogenic elements failed to form. The tympanic ring, which is a BA1 derivative, was not detectable in *Ezh2* cko embryos (Fig. 3E-H). Moreover, analysis at higher magnification revealed that the styloid process, a BA2 derivative, failed to form properly in *Ezh2* cko embryos (Fig. 3G,H). Likewise, the hyoid bone, a BA2 and BA3 derivative, was missing upon *Ezh2* conditional inactivation, as demonstrated by combined staining for Alcian Blue and Eosin on sagittal sections of embryos at E17.5 (Fig. 3I,J). Thus, loss of Ezh2-mediated H3K27me3 appears to interfere with the formation of multiple skeletal elements originating from the NC.

Cell cycle properties and MPC generation are unaffected upon *Ezh2* inactivation

One defining criteria for stem/progenitor cells is their self-renewal capacity. Ezh2 is known to contribute to cell cycle regulation in different cell types, including cancer cells (Pasini et al., 2004). We analyzed the cell cycle properties of MPCs present in the BAs of *Ezh2* cko mice. First, cells undergoing S phase were examined by

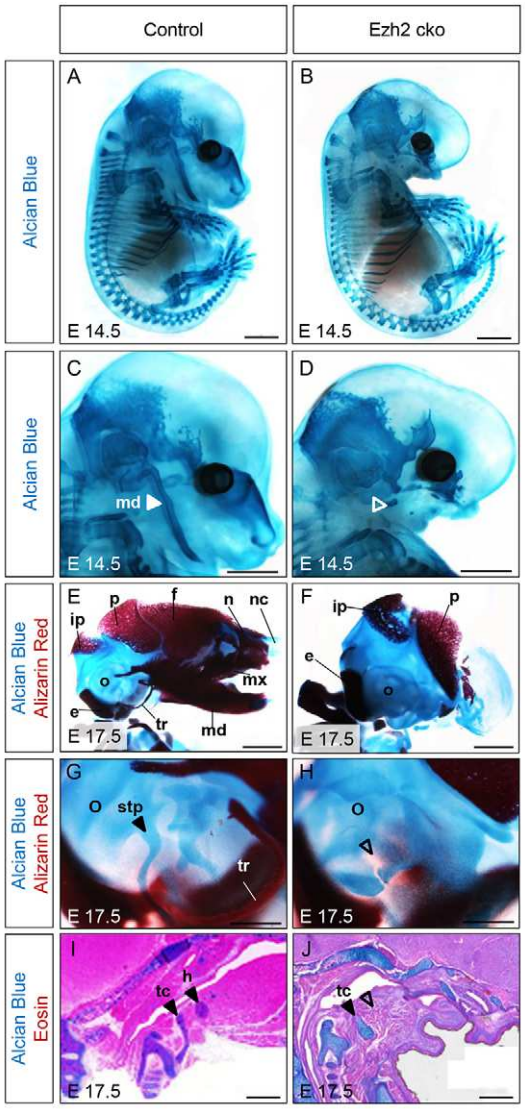

Fig. 3. Skeletal analysis reveals a severe craniofacial defect in *Ezh2* cko embryos. (A-D) Analysis of cartilage formation in control and *Ezh2* cko littermate embryos at E14.5 by Alcian Blue staining. No chondrogenic malformations are observed in the trunk region of *Ezh2* cko embryos compared with control embryos. However, the CNC-derived structures are mostly missing in *Ezh2* cko embryos. (C,D) Higher magnification of the head region of the embryos shown in A and B, highlighting the absence of CNC-derived craniofacial structures in *Ezh2* cko embryos. (E,F) A comparison between control and *Ezh2* cko embryos at E17.5, with combined staining for Alcian Blue and Alizarin Red, shows that craniofacial bone elements are missing in *Ezh2* cko embryos. Head skeleton structures built by mesodermal cells (rather than exclusively by CNCCs) are disturbed, but not entirely missing, whereas structures exclusively originating from CNCCs are missing completely. (G,H) Comparison at higher magnification of the embryos shown in E and F reveals that the styloid process, which is a BA2 derivative, is missing in *Ezh2* cko embryos, as indicated by the open arrowhead. (I,J) Combined staining for Alcian Blue and Eosin in sagittal sections suggested that the hyoid bone, a BA2 and BA3 derivative, is missing in *Ezh2* cko embryos, as indicated by the open arrowhead. ip, interparietal plate; e, exoccipital; nc, nasal capsule; o, otic capsule; p, parietal plate; f, frontal plate; n, nasal plate; mx, maxillary; md, mandible; tr, tympanic ring; stp, styloid process; tc, thyroid cartilage; h, hyoid bone. Scale bars: 2 mm in A-H; 0.5 mm in I,J.

EdU pulse labeling 1 hour prior to euthanization at E11.5 (Fig. 4A). Quantification showed no significant differences in the number of cells that were positive for EdU in BA1 when comparing control

Development (2014) doi:10.1242/dev.094342

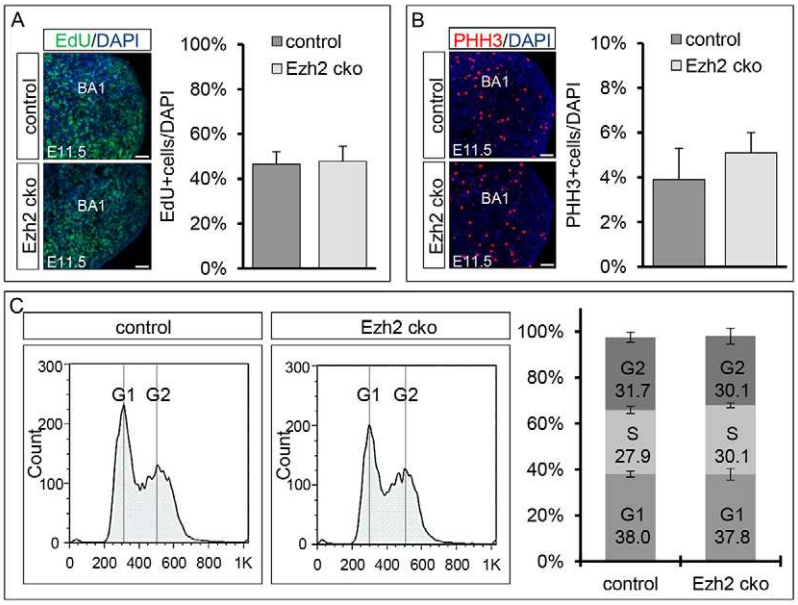

Fig. 4. Cell cycle properties of mesenchymal progenitor cells. (A) Quantification of EdU$^+$ cells in BA1 shows no significant differences between control and *Ezh2* cko littermates. (B) Quantification of mitotic cells assessed by PHH3 immunostaining revealed no significant differences between control and *Ezh2* cko embryos. (C) Cell cycle FACS analysis shows similar profiles for isolated BA1 cells from E11.5 control and *Ezh2* cko littermates. No significant differences were detected for the proportion of cells in different phases of the cell cycle. The S phase cells of both cell cycle profiles were computed with FlowJo and the Fox-Dean-Jett algorithm. Bar charts show mean ± s.e.m. Scale bars: 50 µm.

with *Ezh2* cko mice (46.6% versus 47.8% of cells EdU positive, respectively). Therefore, S phase entry and exit were unaffected in cells lacking *Ezh2*. Next, the number of cells in M phase was determined by phospho-histone H3 (PHH3) immunohistochemical staining (Fig. 4B) on BA1 sections of embryos at E11.5. Again, no significant differences were found between control and *Ezh2* cko animals. BA1 of control and *Ezh2* cko animals contained 3.9% and 5.1% PHH3-positive cells, respectively.

To definitively exclude any cell cycle differences between control and *Ezh2* cko MPCs, we performed cell cycle FACS on cells isolated from BA1 at E11.5. The cell cycle profiles of control and *Ezh2* cko cells were very similar (Fig. 4C). Moreover, no significant changes in cell cycle progression were detected when the proportions of cells in different cell cycle phases were calculated for control and *Ezh2* cko embryos at E11.5. For both genotypes, we found ~31% of the cells in G2 phase and ~38% in G1 phase. Calculations based on cell cycle FACS further indicated the proportion of cells in S phase to be ~30% in both cases.

Overall, these results demonstrate that conditional *Ezh2* inactivation does not change the cell cycle properties of BA cells, suggesting that the observed phenotype is not caused by cell cycle misregulation. Additionally, we did not see differences in the rates of apoptosis between *Ezh2* cko and control embryos at any time point analyzed (data not shown). Thus, the malformations of craniofacial bone and cartilage in *Ezh2* cko animals are due to a deficit in Ezh2 functions other than those regulating cell proliferation and survival.

Ezh2 promotes bone and cartilage formation in CNCCs by repressing inhibitors of an osteochondrogenic program

We previously demonstrated that the transition from NCSCs, emigrating from the hindbrain region to populate the BAs, to MPCs with an osteochondrogenic potential requires the downregulation of the NCSC transcription factor Sox10 and the simultaneous upregulation of the MPC marker Sox9 (John et al., 2011). Therefore, the craniofacial phenotype observed in *Ezh2* cko embryos could be due to a failure of NCSCs to become MPCs. To address this possibility, we performed immunohistochemical analyses of Sox10$^+$ and Sox9$^+$ cells in BA1 of control and *Ezh2* cko embryos at E11.5. Sox10 was restricted to a few cells, which were unaltered in number in *Ezh2* cko as compared with control embryos (Fig. 5A,B,E). Co-staining for NF160 suggested that these Sox10$^+$ cells were putative neural cells associated with nerves in the BA. Unlike Sox10, Sox9 was broadly expressed in both control and mutant BAs, and the number of Sox9$^+$ cells was also unaffected by the inactivation of *Ezh2* (Fig. 5C-E). Furthermore, quantitative RT-PCR in isolated BA1 cells did not reveal any statistically significant differences in the expression of *Sox10* and *Sox9* between *Ezh2* cko embryos and control littermates (Fig. 5F). Thus, MPCs can apparently form in the absence of Ezh2 activity.

Next, we investigated whether MPCs lacking *Ezh2* are able to acquire an osteochondrogenic fate. Immunohistochemical analysis at E11.5 demonstrated that collagen 2a1 (Col2a1) expression, an early indicator of chondrogenic differentiation, was absent in BA1 of *Ezh2* cko embryos, in contrast to control littermates (Fig. 5G,H). Similarly, expression analysis of early markers of osteogenic and chondrogenic differentiation revealed that the transcription factors Runx2 and Osterix (Sp7 – Mouse Genome Informatics), as well as the osteoblast marker alkaline phosphatase (ALP) (Nishimura et al., 2012; Oh et al., 2012), were significantly downregulated in *Ezh2* cko compared with control BA1, as shown by quantitative RT-PCR (Fig. 5I). In summary, MPCs with normal cell cycle properties and a normal Sox factor expression code can be established from NCSCs lacking *Ezh2*. However, conditional ablation of *Ezh2* prevents the early steps of the osteochondrogenic differentiation program in MPCs.

To determine possible mechanisms underlying impaired chondrogenic and skeletogenic differentiation in *Ezh2* cko NC derivatives, we sought to identify putative Ezh2 target genes. BA1 from control and mutant E11.5 embryos was mechanically dissected and total RNA isolated. The Affymetrix A430 microarray platform was then used to perform a differential expression analysis of control versus *Ezh2* cko BA1 cells (Fig. 6A). Clustering of biological replicates demonstrated highly comparable global gene expression patterns among the same genotypes, as shown by a heat map of genes that were at least 2-fold up- or downregulated with $P<0.01$ (Fig. 6B). Since Ezh2 acts as a repressor (Margueron et al., 2008), we focused our analysis

Development (2014) doi:10.1242/dev.094342

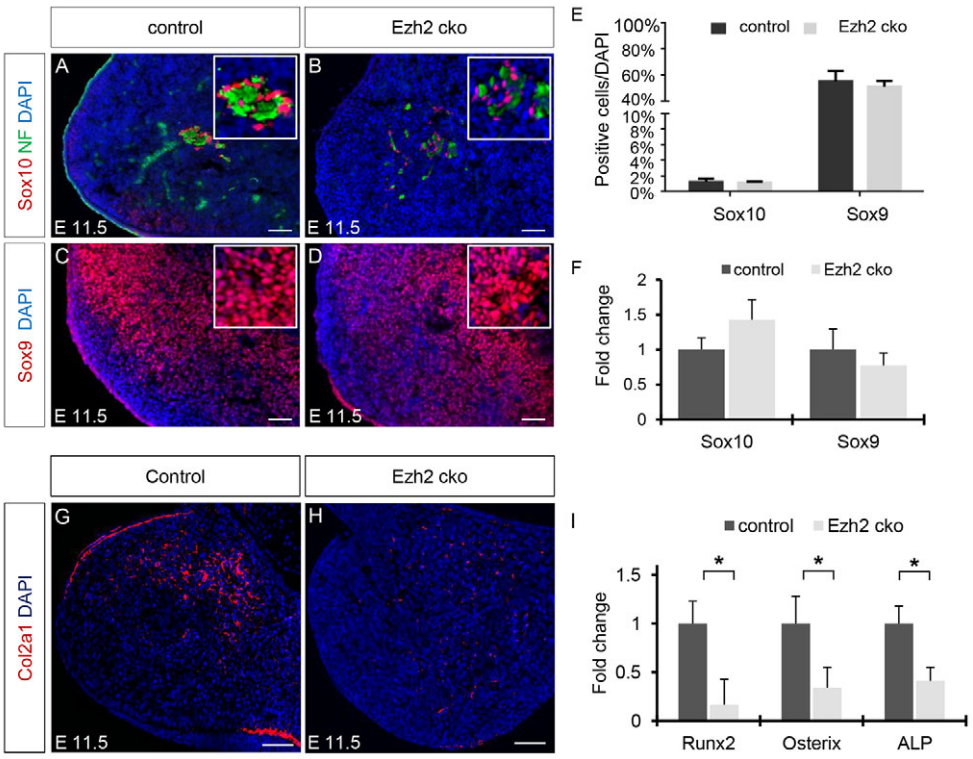

Fig. 5. Osteochondrogenic progenitor establishment and differentiation are impaired in *Ezh2* cko mice. (A-D) Immunohistochemistry reveals that, by E11.5, both control and *Ezh2* cko BA1 cells have lost the expression of the NCSC marker Sox10 and acquired the expression of the mesenchymal progenitor marker Sox9. The few remaining Sox10^{+} cells are associated with nerves, as evidenced by neurofilament (NF) staining (A,B). (E) Quantification of Sox10^{+} and Sox9^{+} cells in BA1 revealed no significant differences between control and *Ezh2* cko embryos. Data are the mean percentage of positive cells/DAPI ± s.e.m. (F) Quantitative RT-PCR in E11.5 control and *Ezh2* cko BA1 cells shows no significant change in the mRNA expression of *Sox10* and *Sox9*. Data are presented as mean fold change ± s.e.m. (G,H) Immunohistochemistry shows the absence of chondrocyte marker Col2a1 expression in *Ezh2* cko BA1 cells. (I) Quantitative RT-PCR for chondro/osteogenesis markers expressed at different stages of chondro/osteogenic differentiation, showing impaired chondro/osteoblast establishment. The expression differences in BA1 cells of control and *Ezh2* cko littermates were significant (*P<0.05). Data are presented as mean fold change ± s.e.m. Scale bars: 50 μm.

on the transcripts upregulated in *Ezh2* cko cells. Strikingly, the expression levels of many Hox gene transcripts were increased in *Ezh2* cko BA1 cells, as particularly evident when a low P-value (P<0.001) was applied to reveal highly significant differences between control cells and cells devoid of *Ezh2* (Table 1). These data were corroborated when we increased the P-value (P<0.05) and found that, with these parameters, 36 out of 39 Hox genes present on the array were upregulated in *Ezh2* cko BA1 cells (data not shown). The overexpression of Hox genes in mutant cells is consistent with the described function of the polycomb group (PcG) complexes in regulating Hox gene expression during embryonic limb and tail development in mice (Soshnikova and Duboule, 2009; Wyngaarden et al., 2011). Moreover, several of the upregulated Hox genes are known to play a role in modulating osteochondrogenic differentiation in different cellular contexts (see Table 1). In our transcriptome analysis, Hox gene expression was upregulated to varying degrees in BA1 cells from *Ezh2* cko embryos as compared with BA1 cells from control littermates (Table 1). Highly elevated expression levels in *Ezh2* cko BAs were also readily detectable by *in situ* hybridization on sections of E11.5 control and mutant embryos (supplementary material Fig. S2A-F; Table S4). To validate these results, we performed quantitative RT-PCR and confirmed the significant increase in expression (P<0.001) of selected Hox genes in *Ezh2* cko versus control BA1 cells (Fig. 6C). Of note, equivalent expression analysis for the same genes failed to show broadly increased expression of Hox genes in the trunk of *Ezh2* cko (supplementary material Fig. S2G), suggesting that Hox gene derepression following loss of *Ezh2* activity is restricted to cranial NC derivatives.

To address whether Hox genes are direct targets of Ezh2-mediated H3K27 trimethylation in BA1 cells, rather than being upregulated due to secondary effects, we performed chromatin immunoprecipitation (ChIP) for H3K27me3 and measured the abundance of DNA occupied by H3K27me3 with primers targeting the transcription start sites of the selected Hox genes. Int1, which is an intergenic region devoid of H3K27me3, was used as a negative control. All of the Hox genes analyzed were found to be modified by H3K27me3 in BA1 cells (Fig. 6D). Thus, multiple Hox genes are direct targets of Ezh2-mediated H3K27me3 in wild-type BA1 cells. Hence, the conditional depletion of *Ezh2* leads to the derepression of many Hox genes, thereby activating numerous well-established suppressors of osteochondrogenesis.

DISCUSSION

In the present study we demonstrate that the PcG protein Ezh2 is a key regulator of CNCC development and is crucial for CNCCs to acquire a chondrogenic and osteogenic fate. Indeed, *Ezh2* conditional ablation and concomitant loss of Ezh2-mediated H3K27 trimethylation in the NC resulted in agenesis of all NC-derived craniofacial structures. Surprisingly, however, *Ezh2* inactivation in

Development (2014) doi:10.1242/dev.094342

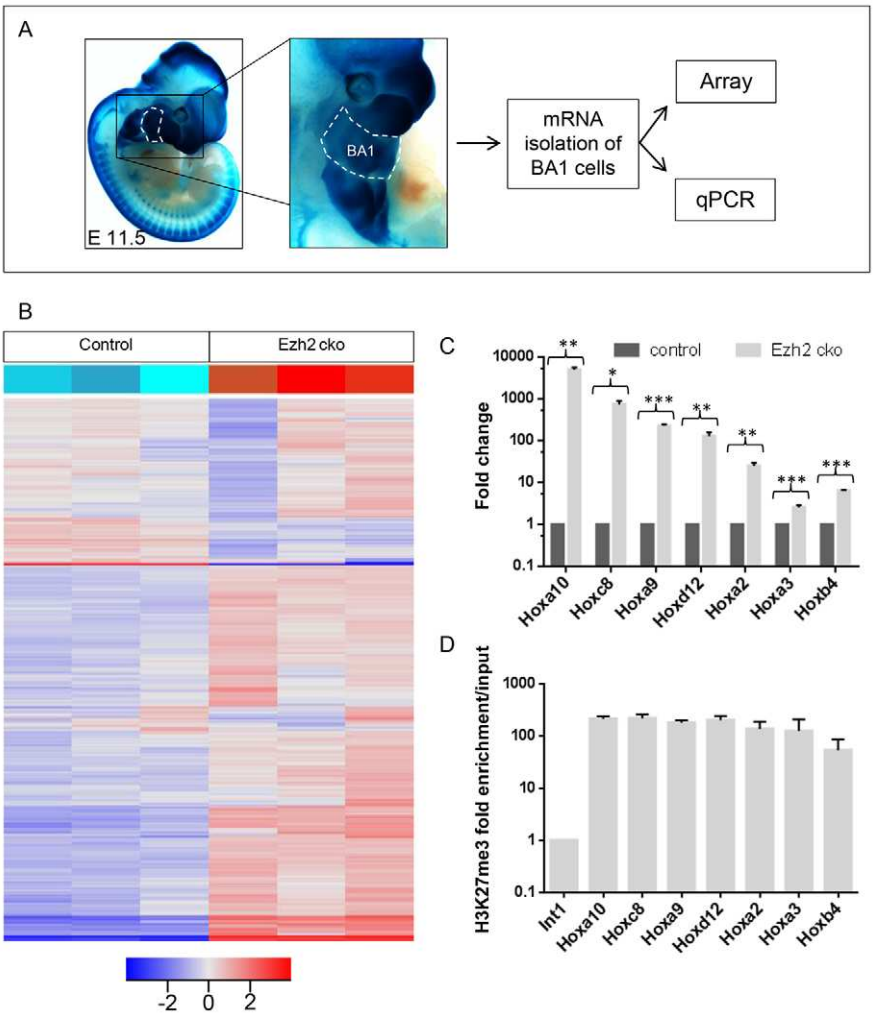

Fig. 6. Hox family genes suppressing osteochondrogenesis are Ezh2 targets and strongly upregulated upon *Ezh2* inactivation. An illustration of the workflow for isolation of BA1 cells from E11.5 control and *Ezh2* cko embryos for microarray and RT-PCR expression analysis. (B) Microarray gene expression heat map of BA1 cells isolated from control and *Ezh2* cko littermates. The signature used in the heat map was compiled from Affymetrix probe sets and shows transcripts that are differentially expressed when applying a fold change of at least 2-fold with $P<0.01$. (C) Quantitative RT-PCR for seven selected Hox genes. BA1 cells of *Ezh2* cko embryos showed significantly higher Hox gene expression than control BA1 cells, suggesting Hox derepression in *Ezh2* cko embryos. Data are presented as mean of fold change ± s.e.m. ***$P<0.001$, **$P<0.01$, *$P<0.05$. (D) ChIP performed to confirm H3K27me3 occupancy in a region around the transcription start site (±500 bp) of selected Hox genes in isolated chromatin from BA1 cells of E11.5 embryos. Data are presented as mean of fold enrichment over input ± s.e.m.

the NC did not cause any overt glial or neuronal defects in the PNS, indicating distinct requirements of epigenetic control mechanisms by different NCC lineages. The only cells with an NC origin that are capable of giving rise to craniofacial skeletal elements are located anterior to or in BA1, BA2, BA3 and BA4. Previously, it has been shown that the capacity of BA1 cells for osteochondrogenesis is dependent on the absence of Hox gene expression (Minoux et al., 2009). As shown here, conditional deletion of *Ezh2* in the NC led to strong upregulation and misexpression of multiple Hox genes in BA cells. Furthermore, we identified Hox genes as direct targets of H3K27me3-dependent transcriptional repression in CNCCs. Thus, the derepression of multiple Hox genes appears to play a major role in preventing osteochondrogenesis in NCCs lacking *Ezh2*. Our findings reveal a crucial role of epigenetic gene silencing in regulating the formation of the jaw and other craniofacial skeletal elements from NCCs.

NCSC proliferation and PNS formation appear not to be affected upon conditional *Ezh2* inactivation

Ezh2 has been indicated as a modulator of cell cycle progression (Chen et al., 2010; Kaneko et al., 2010; Zeng et al., 2011) and controls the maintenance and proliferation of a variety of stem cell types in normal tissue and cancer (Bracken et al., 2006; Ezhkova et al., 2009; Herrera-Merchan et al., 2012; Juan et al., 2011; McCabe et al., 2012; Pereira et al., 2010; Qi et al., 2012; Suvà et al., 2009). By contrast, the number of NCCs emigrating from the neural tube and localizing to NC target structures was not subject to Ezh2-dependent regulation. In fact, NC-specific *Ezh2* ablation did not result in any changes in the cell cycle profile of NC-derived cells. These results indicate that the function of Ezh2 as a cell cycle modulator is tissue specific. Moreover, our data reveal that Ezh2 has a major role in NCCs at relatively late stages of NC development, after NC specification and migration.

Surprisingly, loss of Ezh2 in NCCs also appeared not to affect the formation of neurons and glia in peripheral ganglia and nerves. This is somewhat different to the situation in the CNS, where Ezh2 controls the choice between proliferation and neuronal differentiation, as well as the timely fate switch from neurogenesis to gliogenesis (Hirabayashi et al., 2009; Pereira et al., 2010). By contrast, dorsal root and autonomic ganglia of *Ezh2* cko embryos contained normal numbers of sensory and autonomic neurons, respectively. Likewise, differentiation and the timely appearance of satellite glia in ganglia and Schwann cells along peripheral nerves were unaffected in *Ezh2* cko compared with control embryos. Taken together, the generation and differentiation of neural lineages from NCCs are apparently not dependent on Ezh2-mediated epigenetic gene regulation. Interestingly, Shen and colleagues (Shen et al., 2008) have previously reported lineage-specific requirements for Ezh2 during differentiation of mESCs. *Ezh2* ablation in ESCs induced neural/ectoderm lineages at the expense of the mesodermal

Development (2014) doi:10.1242/dev.094342

and endodermal differentiation programs. This suggests that the endodermal and mesodermal lineages are more susceptible to changes in Ezh2 activity than are neural lineages (Shen et al., 2008). Our findings are consistent with this hypothesis: neural lineage formation remained unaffected upon inactivation of *Ezh2* in the NC, whereas the development of NC-derived mesenchymal progenitors, which adopt a differentiation program similar to that of the mesoderm *in vivo*, was severely hampered in mutant mice.

An alternative explanation for unimpaired PNS development in *Ezh2* cko embryos is that, in the PNS, Ezh1 activity might compensate for the loss of Ezh2 by catalyzing the methylation mark on H3K27, but fails to do so in cranial NC-derived MPCs. Others have previously demonstrated that, upon loss of *Ezh2*, Ezh1 can take over the catalytic function of Ezh2 for a particular subset of genes crucial for development (Boyer et al., 2006; Ezhkova et al., 2011). However, in the present study, conditional deletion of *Ezh2* was accompanied by a major loss of H3K27me3 in migratory trunk NCCs at early developmental stages and in all NC derivatives analyzed, including PNS structures, suggesting that Ezh1 was unable to assume Ezh2 functions in a global manner in mutant NCCs. Nonetheless, we cannot rule out that a subset of genes crucial for neurogenesis remains occupied by H3K27me3 in *Ezh2* cko embryos due to Ezh1 compensation, allowing for normal PNS development. Furthermore, distinct epigenetic silencing mechanisms (e.g. H3K9 trimethylation and/or DNA methylation, in addition to H3K27 trimethylation) might have redundant functions in repressing gene expression during PNS development. Conceivably, however, loss of Ezh2 and H3K27me3 leads to gene derepression also in the PNS, but these genes encode factors that apparently do not interfere with neuronal and glial differentiation programs when overexpressed.

Ezh2 is required for craniofacial chondrogenesis and osteogenesis

In contrast to PNS development, Ezh2 activity is indispensable for osteochondrogenesis and thus for the formation of the craniofacial skeletal elements originating from the NC. During development, NCSCs originating in the cranial NC undergo a transition to MPCs, thereby losing neural potential and, at the same time, gaining the potential to produce mesenchymal lineages (John et al., 2011). This developmental switch is characterized by downregulation of the transcription factor Sox10 and concomitant upregulation of the transcription factor Sox9. Sox9 has been implicated in craniofacial development (Mori-Akiyama et al., 2003), although its conditional ablation in the NC resulted in a much less severe phenotype than exhibited by *Ezh2* cko embryos. One possible explanation for the craniofacial phenotype observed upon *Ezh2* ablation is a failure of mutant NCSCs to give rise to MPCs. However, analysis of Sox9 and Sox10 expression levels did not reveal statistically significant changes upon *Ezh2* inactivation. By contrast, early stages of chondrogenesis were impaired in *Ezh2* cko embryos, as indicated by the lack of Col2a1 in mutant BA cells. Additionally, other chondrogenic and osteogenic markers, such as Runx2, Osterix and ALP, failed to be expressed by BA cells upon *Ezh2* deletion. Our findings show that MPC identity can be established in the absence of Ezh2-mediated H3K27me3. However, *Ezh2* inactivation prevents MPCs from acquiring an osteochondrogenic fate and, hence, producing cartilage and bone.

Ezh2 activity silences Hox gene expression in CNCCs

Craniofacial skeletal elements originating from the NC are exclusively produced from areas anterior to or located in BA1, BA2, BA3 and BA4, and NCCs posterior to these structures do not give rise to cartilage or bone. Moreover, CNCCs that populate the BA1 and the nasofrontal areas must have a Homeobox-free ground pattern to undergo both forms of osteogenesis, i.e. endochondral and intramembranous ossification (Santagati and Rijli, 2003; Kanzler et al., 1998). BA2 cells express a single Hox gene, *Hoxa2*, and only undergo endochondral ossification (Kanzler et al., 1998; Minoux et al., 2009; Santagati and Rijli, 2003). NCCs more caudal to BA2 are characterized by expression of several Hox genes and display a well-defined Hox gene expression code that varies according to the anterior-posterior position. Many Hox factors have been shown to suppress osteochondrogenesis, hence restricting this potential to anterior NC populations (Couly et al., 1998; Kanzler et al., 1998; Yueh et al., 1998; Creuzet et al., 2002).

Large-scale analysis of ESCs has previously shown that Ezh2 occupancy, although widespread in the genome, is not global, but

Table 1. Hox gene derepression in *Ezh2* cko BA1 cells

Gene symbol	Ratio	*P*-value	References
Hoxa9	134.3	1.43×10^{-9}	Shi et al., 2001
Hoxa10	104.2	1.79×10^{-11}	Hassan et al., 2007
Hoxc8	56.2	3.12×10^{-9}	Yueh et al., 1998
Hoxb3	21.7	3.11×10^{-8}	Manley and Capecchi, 1997
Hoxd13	21.5	1.01×10^{-8}	Chae et al., 2008
Hoxc10	15.4	7.08×10^{-6}	Hostikka et al., 2009
Hoxc4	12.1	4.17×10^{-8}	
Hoxa11	10.5	2.14×10^{-6}	Gross et al., 2012
Hoxb13	10.2	4.03×10^{-7}	
Hoxa2	8.5	3.14×10^{-8}	Kanzler et al., 1998; Couly et al., 1998; Creuzet et al., 2002
Hoxa5	5.0	1.51×10^{-4}	
Hoxc9	4.3	1.78×10^{-8}	
Hoxa3	4.1	1.23×10^{-4}	Creuzet et al., 2002; Manley and Capecchi, 1997
Hoxc5	3.5	6.58×10^{-6}	
Hoxc13	2.6	2.73×10^{-5}	Chae et al., 2008
Hoxd8	2.5	4.62×10^{-5}	
Hoxa1	2.4	1.21×10^{-6}	
Hoxb2	2.1	2.22×10^{-5}	
Hoxa7	2.1	6.43×10^{-6}	
Hoxb4	2.0	1.12×10^{-4}	Couly et al., 1998; Creuzet et al., 2002

Hox genes from the microarray that are derepressed in *Ezh2* cko BA1 cells in a highly significant manner, with upregulation of at least 2-fold and $P<0.001$. References are listed that describe an involvement of the respective Hox gene in chondrogenesis or osteogenesis. *Hoxa2*, *Hoxa3* and *Hoxb4* have been described to block skeletogenesis specifically in CNCCs.

Development (2014) doi:10.1242/dev.094342

rather is mostly associated with development-related genes (Boyer et al., 2006). Among these, the Hox gene cluster was found to be prominently regulated by Ezh2 in ESCs. Likewise, Hox genes are well-established targets of polycomb regulation in *Drosophila* (Ringrose and Paro, 2004; Sparmann and van Lohuizen, 2006). Interestingly, our microarray analysis demonstrated that, also in BA1 cells isolated from *Ezh2* cko embryos, many Hox genes are heavily upregulated when compared with control embryos. Therefore, massive Hox gene misexpression, probably in conjunction with misregulation of other Ezh2 target genes, might be a major cause of the craniofacial defects observed upon loss of Ezh2 and H3K27me3 in NCCs.

Indeed, several reports have suggested that erratic Hox gene expression causes impaired chondrogenesis and osteogenesis. For instance, Hoxa2, which is overexpressed in BA1 cells of *Ezh2* cko embryos, is a well-known inhibitor of intramembranous bone formation from BAs, and when overexpressed in the Hox-negative domain of avian embryos impairs formation of the facial skeleton (Couly et al., 1998; Creuzet et al., 2002; Kanzler et al., 1998). Massip and colleagues have shown that ectopic expression of Hoxa2 in chondrocytes results in impaired differentiation, as demonstrated by the lack of Col2a1, and prevents cartilage formation (Massip et al., 2007). In BA2, Hoxa2 is a promoter of the hyoid fate of mesenchymal CNCCs and restricts the chondrogenic domains that arise during endochondral ossification (Pasqualetti et al., 2000). Hoxa2 gain-of-function in BA1 cells results in a duplication of BA2 skeletal elements in *Xenopus* (Pasqualetti et al., 2000), whereas Hoxa2 loss in BA2 in mice leads to a mirror homeotic transformation of BA1 skeletal elements (Rijli et al., 1993). Importantly, Hoxa2 in BA2 prevents osteogenesis by blocking its main effector, Runx2. In addition, Hoxa2 is also involved in cartilage patterning until E11.5 by an independent mechanism that involves different co-factors. Conditional gene inactivation further revealed that subpopulations of CNCCs require Hoxa2 at defined time points for proper BA patterning (Santagati et al., 2005). Hoxc8 is another factor that prevents endochondral differentiation by maintaining chondrocytes in a proliferative state and inhibiting chondrocyte hypertrophy (Yueh et al., 1998). Furthermore, Hoxa9 is known to be a direct repressor of the earlier bone inducer osteopontin in lung epithelial cell lines (Shi et al., 2001). Interestingly, Hoxa10 contributes to the onset and maintenance of osteogenesis by activating Runx2 and osteoblast-specific genes (Hassan et al., 2007). Finally, Hoxa3 and Hoxb4 are also well-known inhibitors of osteogenesis in NC precursor cells. When individually overexpressed in NC derivatives of chicken embryos, Hoxa3 expression results in the formation of rudimentary nasofrontal bud derivatives, whereas Hoxb4 impairs terminal differentiation of BA1 derivatives such as the proximal bones (Couly et al., 1998; Creuzet et al., 2002). However, when jointly overexpressed, Hoxa3 and Hoxb4 block skeletogenesis to a similar extent as ectopic Hoxa2 expression.

All these data indicate that NC precursors are specified for osteochondrogenesis in a temporally controlled manner, and that finely tuned regulation of Hox gene expression is crucial for this process. In BAs of *Ezh2* cko embryos, high and ectopic expression of the Hox genes mentioned above to suppress osteogenesis and chondrogenesis, as well as of many other Hox genes, is associated with the inhibition of chondrogenic and osteogenic gene expression programs and a virtually complete blockage of cartilage and bone formation from NCCs. By contrast, *Ezh2* inactivation in trunk NC does not lead to profound changes in Hox gene expression or the overt malformation of neural lineages. Thus, Ezh2-mediated H3K27 trimethylation plays a lineage-specific role in NCCs, repressing Hox genes in anterior NC subpopulations and thus allowing osteochondrogenesis in these cells. Clearly, region-specific Hox gene regulation and the potential to form skeletal structures must involve other factors as well, given that Ezh2 and H3K27me3 are also broadly expressed in more posterior NCCs, which *in vivo* do not form cartilage and bone. These factors include intrinsic cues that distinguish CNCCs from more caudal NCCs, as suggested, for example, by clonal assays in cell culture or by the *in vivo* manipulation of signaling pathways regulating neural and osteochondrogenic fates (Büchmann-Møller et al., 2009; Calloni et al., 2009; John et al., 2011). The nature of these cues and their potential functional interaction with epigenetic regulators, including Ezh2, remain to be determined. Moreover, our study raises the intriguing question of whether and how epigenetic control of osteochondrogenesis in NCCs was involved in the evolution of jawed vertebrates.

MATERIALS AND METHODS

Animals and genotyping

The *Cre-loxP* system was used to conditionally ablate *Ezh2* in NCCs. Mice carrying a transgene, in which two exons encoding the SET domain of *Ezh2* are flanked by *loxP* sites, have been described (Hirabayashi et al., 2009). Homozygous animals ($Ezh2^{lox/lox}$) were crossed with animals carrying the *Wnt1-Cre* transgene (Danielian et al., 1998). Offspring with the genotype *Wnt1-Cre;* $Ezh2^{lox/lox}$ were termed *Ezh2* cko and compared with their respective littermates having either no *Wnt1-Cre* transgene ($Ezh2^{lox/lox}$ or $Ezh2^{lox/wt}$) or lacking a second copy of the floxed *Ezh2* transgene (*Wnt1-Cre,* $Ezh2^{lox/wt}$). Such control animals never showed an overt phenotype and displayed normal life expectancy. Timed matings were performed overnight (o/n) and noon on the following day was considered E0.5. *In vivo* fate mapping of NCCs was performed on mice additionally carrying the *R26R-lacZ* allele (Soriano, 1999). Genotyping was by PCR on genomic DNA obtained from tails. Primers are listed in supplementary material Tables S1 and S1.1. All animal experiments were conducted in accordance with the Veterinary Office of the Canton of Zurich, Switzerland.

Immunohistochemistry, X-Gal staining and EdU staining

For immunohistochemistry, cryosections were processed as previously described (John et al., 2011). Primary antibodies were used as follows: rabbit anti-PHH3 (1:200; Millipore, 06-570), mouse anti-tyrosine hydroxylase (TH) (1:200; Sigma, T1299), mouse anti-Mash1 (1:100; BD Biosciences, 556604), rabbit anti-Brn3a (1:2000; a gift from E. E. Turner, Seattle Children's Research Institute, Seattle, WA, USA), mouse anti-NF160 (1:400; Sigma, N-5264), rabbit anti-NF160 (1:200; Chemicon, AB1987), rabbit anti-Ki67 (1:200; Abcam, ab 15580), rabbit anti-cleaved caspase 3 (1:200; Cell Signaling, 9661), rabbit anti-H3K27me3 (1:200; Millipore, 07-449), rabbit anti-Oct6 (1:200; gift from Dies Meijer, Erasmus University, Rotterdam, The Netherlands), rabbit anti-Col2a1 (1:200; Acris, R1039X), goat anti-Sox10 (1:100; Santa Cruz, sc-17342), rabbit anti-Sox9 (1:50; Santa Cruz, sc-20095) and chicken anti-β-galactosidase (1:200; Abcam, ab 9361). Secondary antibodies were from Jackson ImmunoResearch or Invitrogen. *lacZ* reporter gene expression was detected as previously described (Hari et al., 2012). EdU stainings were performed according to the manufacturer's protocols (Invitrogen). EdU was injected intraperitoneally 1 hour before euthanization of time-mated animals at E11.5.

Isolation and preparation of BA1 cells

BA1 cells were isolated from embryos as described (John et al., 2011). For mRNA isolation (microarray analysis and quantitative RT-PCR) we used the RNeasy Mini Kit (Qiagen). For ChIP we followed the protocol of Weber et al. (Weber et al., 2007).

Cell cycle FACS analysis

Wnt1-Cre; $Ezh2^{lox/lox}$ and $Ezh2^{lox/lox}$ BA1 cells were taken up in 500 µl PBS containing 1.25 mM 5-AAD (Sigma), washed twice in PBS and then

analyzed using a FACS Canto II flow cytometer (BD Biosciences). FlowJo software (Tree Star) was used to analyze the data and for quantification. The quantification (Fig. 4D) was performed with the Dean-Jett-Fox algorithm (Fox, 1980) provided by FlowJo.

Quantitative RT-PCR and ChIP-quantitative PCR

Total mRNA (0.5 µg) from BA1 cells served as template for reverse transcription with oligo(dT) primers (Invitrogen) and superscript III reverse transcriptase (Invitrogen). The quantitative PCR reaction was performed on a LightCycler II (Roche). For ChIP samples, 1 µl of ChIP samples or input DNA was used per PCR reaction. Each experiment was performed in triplicate and three independent quantitative PCR reactions were then analyzed using the ΔCt method. β-actin was used for normalization. Primers are listed in supplementary material Tables S2 and S3.

Alcian Blue and Alizarin Red staining

Alcian Blue (Fluka) and Alizarin Red (Chroma) stainings followed published protocols (Nagy, 2003).

Microarray

After mRNA extraction we submitted the samples to the Functional Genomics Center Zurich (FGCZ) for processing. The Affymetrix A430 platform was used to compare transcriptional differences between *Wnt1-Cre; Ezh2*$^{lox/lox}$ and *Ezh2*$^{lox/lox}$ BA1 cells. The array was uploaded to Gene Expression Omnibus with accession number GSE52220.

Statistical analyses

Each experiment was performed using at least three different embryos. Statistical significance was tested with an unpaired, two-tailed Student's *t*-test.

Acknowledgements

We thank Michal Okoniewski, Max Gay and Jessica Häusel for help with microarray analysis, *in situ* hybridization experiments and technical assistance, respectively.

Competing interests

The authors declare no competing financial interests.

Author contributions

D. Schwarz, S.V., D. Schübeler and L.S. designed the experiments; D. Schwarz, S.V., M.Z., A.S., A.B. and K.D. performed the experiments; D. Schwarz, S.V., M.Z. and A.S. analyzed the data; H.K. provided the *Ezh2*$^{fl/fl}$ mouse line; D. Schwarz, S.V. and L.S. wrote the manuscript.

Funding

This work was supported by the Swiss National Science Foundation, including a Sinergia Grant (to D. Schübeler and L.S.); The University Research Priority Program (URPP) 'Translational Cancer Research' (to S.V.); and the National Research Program (NRP63) 'Stem Cells and Regenerative Medicine'.

Supplementary material

Supplementary material available online at
http://dev.biologists.org/lookup/suppl/doi:10.1242/dev.094342/-/DC1

References

Boyer, L. A., Plath, K., Zeitlinger, J., Brambrink, T., Medeiros, L. A., Lee, T. I., Levine, S. S., Wernig, M., Tajonar, A., Ray, M. K. et al. (2006). Polycomb complexes repress developmental regulators in murine embryonic stem cells. *Nature* **441**, 349-353.

Bracken, A. P., Dietrich, N., Pasini, D., Hansen, K. H. and Helin, K. (2006). Genome-wide mapping of Polycomb target genes unravels their roles in cell fate transitions. *Genes Dev.* **20**, 1123-1136.

Büchmann-Møller, S., Miescher, I., John, N., Krishnan, J., Deng, C. X. and Sommer, L. (2009). Multiple lineage-specific roles of Smad4 during neural crest development. *Dev. Biol.* **330**, 329-338.

Calloni, G. W., Le Douarin, N. M. and Dupin, E. (2009). High frequency of cephalic neural crest cells shows coexistence of neurogenic, melanogenic, and osteogenic differentiation capacities. *Proc. Natl. Acad. Sci. USA* **106**, 8947-8952.

Chae, S. W., Jee, B. K., Lee, J. Y., Han, C. W., Jeon, Y. W., Lim, Y., Lee, K. H., Rha, H. K. and Chae, G. T. (2008). HOX gene analysis in the osteogenic differentiation of human mesenchymal stem cells. *Genet. Mol. Biol.* **31**, 815-823.

Chai, Y., Jiang, X., Ito, Y., Bringas, P., Jr, Han, J., Rowitch, D. H., Soriano, P., McMahon, A. P. and Sucov, H. M. (2000). Fate of the mammalian cranial neural crest during tooth and mandibular morphogenesis. *Development* **127**, 1671-1679.

Chen, S., Bohrer, L. R., Rai, A. N., Pan, Y., Gan, L., Zhou, X., Bagchi, A., Simon, J. A. and Huang, H. (2010). Cyclin-dependent kinases regulate epigenetic gene silencing through phosphorylation of EZH2. *Nat. Cell Biol.* **12**, 1108-1114.

Couly, G., Grapin-Botton, A., Coltey, P., Ruhin, B. and Le Douarin, N. M. (1998). Determination of the identity of the derivatives of the cephalic neural crest: incompatibility between Hox gene expression and lower jaw development. *Development* **125**, 3445-3459.

Creuzet, S., Couly, G., Vincent, C. and Le Douarin, N. M. (2002). Negative effect of Hox gene expression on the development of the neural crest-derived facial skeleton. *Development* **129**, 4301-4313.

Danielian, P. S., Muccino, D., Rowitch, D. H., Michael, S. K. and McMahon, A. P. (1998). Modification of gene activity in mouse embryos in utero by a tamoxifen-inducible form of Cre recombinase. *Curr. Biol.* **8**, 1323-S2.

Eng, S. R., Lanier, J., Fedtsova, N. and Turner, E. E. (2004). Coordinated regulation of gene expression by Brn3a in developing sensory ganglia. *Development* **131**, 3859-3870.

Ezhkova, E., Pasolli, H. A., Parker, J. S., Stokes, N., Su, I. H., Hannon, G., Tarakhovsky, A. and Fuchs, E. (2009). Ezh2 orchestrates gene expression for the stepwise differentiation of tissue-specific stem cells. *Cell* **136**, 1122-1135.

Ezhkova, E., Lien, W. H., Stokes, N., Pasolli, H. A., Silva, J. M. and Fuchs, E. (2011). EZH1 and EZH2 cogovern histone H3K27 trimethylation and are essential for hair follicle homeostasis and wound repair. *Genes Dev.* **25**, 485-498.

Fox, M. H. (1980). A model for the computer analysis of synchronous DNA distributions obtained by flow cytometry. *Cytometry* **1**, 71-77.

Gammill, L. S. and Bronner-Fraser, M. (2003). Neural crest specification: migrating into genomics. *Nat. Rev. Neurosci.* **4**, 795-805.

Gross, J. B. and Hanken, J. (2008). Review of fate-mapping studies of osteogenic cranial neural crest in vertebrates. *Dev. Biol.* **317**, 389-400.

Gross, S., Krause, Y., Wuelling, M. and Vortkamp, A. (2012). Hoxa11 and Hoxd11 regulate chondrocyte differentiation upstream of Runx2 and Shox2 in mice. *PLoS ONE* **7**, e43553.

Hari, L., Brault, V., Kléber, M., Lee, H. Y., Ille, F., Leimeroth, R., Paratore, C., Suter, U., Kemler, R. and Sommer, L. (2002). Lineage-specific requirements of beta-catenin in neural crest development. *J. Cell Biol.* **159**, 867-880.

Hari, L., Miescher, I., Shakhova, O., Suter, U., Chin, L., Taketo, M., Richardson, W. D., Kessaris, N. and Sommer, L. (2012). Temporal control of neural crest lineage generation by Wnt/β-catenin signaling. *Development* **139**, 2107-2117.

Hassan, M. Q., Tare, R., Lee, S. H., Mandeville, M., Weiner, B., Montecino, M., van Wijnen, A. J., Stein, J. L., Stein, G. S. and Lian, J. B. (2007). HOXA10 controls osteoblastogenesis by directly activating bone regulatory and phenotypic genes. *Mol. Cell. Biol.* **27**, 3337-3352.

Herrera-Merchan, A., Arranz, L., Ligos, J. M., de Molina, A., Dominguez, O. and Gonzalez, S. (2012). Ectopic expression of the histone methyltransferase Ezh2 in haematopoietic stem cells causes myeloproliferative disease. *Nat. Commun.* **3**, 623.

Hirabayashi, Y., Suzki, N., Tsuboi, M., Endo, T. A., Toyoda, T., Shinga, J., Koseki, H., Vidal, M. and Gotoh, Y. (2009). Polycomb limits the neurogenic competence of neural precursor cells to promote astrogenic fate transition. *Neuron* **63**, 600-613.

Hostikka, S. L., Gong, J. and Carpenter, E. M. (2009). Axial and appendicular skeletal transformations, ligament alterations, and motor neuron loss in Hoxc10 mutants. *Int. J. Biol. Sci.* **5**, 397-410.

Jiang, X., Iseki, S., Maxson, R. E., Sucov, H. M. and Morriss-Kay, G. M. (2002). Tissue origins and interactions in the mammalian skull vault. *Dev. Biol.* **241**, 106-116.

John, N., Cinelli, P., Wegner, M. and Sommer, L. (2011). Transforming growth factor β-mediated Sox10 suppression controls mesenchymal progenitor generation in neural crest stem cells. *Stem Cells* **29**, 689-699.

Juan, A. H., Derfoul, A., Feng, X., Ryall, J. G., Dell'Orso, S., Pasut, A., Zare, H., Simone, J. M., Rudnicki, M. A. and Sartorelli, V. (2011). Polycomb EZH2 controls self-renewal and safeguards the transcriptional identity of skeletal muscle stem cells. *Genes Dev.* **25**, 789-794.

Kaneko, S., Li, G., Son, J., Xu, C. F., Margueron, R., Neubert, T. A. and Reinberg, D. (2010). Phosphorylation of the PRC2 component Ezh2 is cell cycle-regulated and up-regulates its binding to ncRNA. *Genes Dev.* **24**, 2615-2620.

Kanzler, B., Kuschert, S. J., Liu, Y. H. and Mallo, M. (1998). Hoxa-2 restricts the chondrogenic domain and inhibits bone formation during development of the branchial area. *Development* **125**, 2587-2597.

Le Douarin, N. M. and Dupin, E. (2012). The neural crest in vertebrate evolution. *Curr. Opin. Genet. Dev.* **22**, 381-389.

Le Douarin, N. M., Brito, J. M. and Creuzet, S. (2007). Role of the neural crest in face and brain development. *Brain Res. Rev.* **55**, 237-247.

Manley, N. R. and Capecchi, M. R. (1997). Hox group 3 paralogous genes act synergistically in the formation of somitic and neural crest-derived structures. *Dev. Biol.* **192**, 274-288.

Margueron, R. and Reinberg, D. (2011). The Polycomb complex PRC2 and its mark in life. *Nature* **469**, 343-349.

Margueron, R., Li, G., Sarma, K., Blais, A., Zavadil, J., Woodcock, C. L., Dynlacht, B. D. and Reinberg, D. (2008). Ezh1 and Ezh2 maintain repressive chromatin through different mechanisms. *Mol. Cell* **32**, 503-518.

Massip, L., Ectors, F., Deprez, P., Maleki, M., Behets, C., Lengelé, B., Delahaut, P., Picard, J. and Rezsöhazy, R. (2007). Expression of Hoxa2 in cells entering chondrogenesis impairs overall cartilage development. *Differentiation* **75**, 256-267.

McCabe, M. T., Graves, A. P., Ganji, G., Diaz, E., Halsey, W. S., Jiang, Y., Smitheman, K. N., Ott, H. M., Pappalardi, M. B., Allen, K. E. et al. (2012).

Mutation of A677 in histone methyltransferase EZH2 in human B-cell lymphoma promotes hypertrimethylation of histone H3 on lysine 27 (H3K27). *Proc. Natl. Acad. Sci. USA* **109**, 2989-2994.
Mikkelsen, T. S., Ku, M., Jaffe, D. B., Issac, B., Lieberman, E., Giannoukos, G., Alvarez, P., Brockman, W., Kim, T. K., Koche, R. P. et al. (2007). Genome-wide maps of chromatin state in pluripotent and lineage-committed cells. *Nature* **448**, 553-560.
Minoux, M. and Rijli, F. M. (2010). Molecular mechanisms of cranial neural crest cell migration and patterning in craniofacial development. *Development* **137**, 2605-2621.
Minoux, M., Antonarakis, G. S., Kmita, M., Duboule, D. and Rijli, F. M. (2009). Rostral and caudal pharyngeal arches share a common neural crest ground pattern. *Development* **136**, 637-645.
Mori-Akiyama, Y., Akiyama, H., Rowitch, D. H. and de Crombrugghe, B. (2003). Sox9 is required for determination of the chondrogenic cell lineage in the cranial neural crest. *Proc. Natl. Acad. Sci. USA* **100**, 9360-9365.
Nagy, A. (2003). *Manipulating the Mouse Embryo: A Laboratory Manual*. Cold Spring Harbor, NY: Cold Spring Harbor Laboratory Press.
Nishimura, R., Hata, K., Matsubara, T., Wakabayashi, M. and Yoneda, T. (2012). Regulation of bone and cartilage development by network between BMP signalling and transcription factors. *J. Biochem.* **151**, 247-254.
O'Carroll, D., Erhardt, S., Pagani, M., Barton, S. C., Surani, M. A. and Jenuwein, T. (2001). The polycomb-group gene Ezh2 is required for early mouse development. *Mol. Cell. Biol.* **21**, 4330-4336.
Oh, J. H., Park, S. Y., de Crombrugghe, B. and Kim, J. E. (2012). Chondrocyte-specific ablation of Osterix leads to impaired endochondral ossification. *Biochem. Biophys. Res. Commun.* **418**, 634-640.
Pasini, D., Bracken, A. P. and Helin, K. (2004). Polycomb group proteins in cell cycle progression and cancer. *Cell Cycle* **3**, 394-398.
Pasqualetti, M., Ori, M., Nardi, I. and Rijli, F. M. (2000). Ectopic Hoxa2 induction after neural crest migration results in homeosis of jaw elements in Xenopus. *Development* **127**, 5367-5378.
Pereira, J. D., Sansom, S. N., Smith, J., Dobenecker, M. W., Tarakhovsky, A. and Livesey, F. J. (2010). Ezh2, the histone methyltransferase of PRC2, regulates the balance between self-renewal and differentiation in the cerebral cortex. *Proc. Natl. Acad. Sci. USA* **107**, 15957-15962.
Qi, W., Chan, H., Teng, L., Li, L., Chuai, S., Zhang, R., Zeng, J., Li, M., Fan, H., Lin, Y. et al. (2012). Selective inhibition of Ezh2 by a small molecule inhibitor blocks tumor cells proliferation. *Proc. Natl. Acad. Sci. USA* **109**, 21360-21365.
Rijli, F. M., Mark, M., Lakkaraju, S., Dierich, A., Dollé, P. and Chambon, P. (1993). A homeotic transformation is generated in the rostral branchial region of the head by disruption of Hoxa-2, which acts as a selector gene. *Cell* **75**, 1333-1349.
Ringrose, L. and Paro, R. (2004). Epigenetic regulation of cellular memory by the Polycomb and Trithorax group proteins. *Annu. Rev. Genet.* **38**, 413-443.
Santagati, F. and Rijli, F. M. (2003). Cranial neural crest and the building of the vertebrate head. *Nat. Rev. Neurosci.* **4**, 806-818.
Santagati, F., Minoux, M., Ren, S. Y. and Rijli, F. M. (2005). Temporal requirement of Hoxa2 in cranial neural crest skeletal morphogenesis. *Development* **132**, 4927-4936.
Schuettengruber, B., Chourrout, D., Vervoort, M., Leblanc, B. and Cavalli, G. (2007). Genome regulation by polycomb and trithorax proteins. *Cell* **128**, 735-745.
Shen, X., Liu, Y., Hsu, Y. J., Fujiwara, Y., Kim, J., Mao, X., Yuan, G. C. and Orkin, S. H. (2008). EZH1 mediates methylation on histone H3 lysine 27 and complements EZH2 in maintaining stem cell identity and executing pluripotency. *Mol. Cell* **32**, 491-502.
Shi, X., Bai, S., Li, L. and Cao, X. (2001). Hoxa-9 represses transforming growth factor-beta-induced osteopontin gene transcription. *J. Biol. Chem.* **276**, 850-855.
Sommer, L. (2011). Generation of melanocytes from neural crest cells. *Pigment Cell Melanoma Res.* **24**, 411-421.
Soriano, P. (1999). Generalized lacZ expression with the ROSA26 Cre reporter strain. *Nat. Genet.* **21**, 70-71.
Soshnikova, N. and Duboule, D. (2009). Epigenetic temporal control of mouse Hox genes in vivo. *Science* **324**, 1320-1323.
Sparmann, A. and van Lohuizen, M. (2006). Polycomb silencers control cell fate, development and cancer. *Nat. Rev. Cancer* **6**, 846-856.
Strobl-Mazzulla, P. H., Sauka-Spengler, T. and Bronner-Fraser, M. (2010). Histone demethylase JmjD2A regulates neural crest specification. *Dev. Cell* **19**, 460-468.
Suvà, M. L., Riggi, N., Janiszewska, M., Radovanovic, I., Provero, P., Stehle, J. C., Baumer, K., Le Bitoux, M. A., Marino, D., Cironi, L. et al. (2009). EZH2 is essential for glioblastoma cancer stem cell maintenance. *Cancer Res.* **69**, 9211-9218.
Weber, M., Hellmann, I., Stadler, M. B., Ramos, L., Pääbo, S., Rebhan, M. and Schübeler, D. (2007). Distribution, silencing potential and evolutionary impact of promoter DNA methylation in the human genome. *Nat. Genet.* **39**, 457-466.
Wurdak, H., Ittner, L. M., Lang, K. S., Leveen, P., Suter, U., Fischer, J. A., Karlsson, S., Born, W. and Sommer, L. (2005). Inactivation of TGFbeta signaling in neural crest stem cells leads to multiple defects reminiscent of DiGeorge syndrome. *Genes Dev.* **19**, 530-535.
Wurdak, H., Ittner, L. M. and Sommer, L. (2006). DiGeorge syndrome and pharyngeal apparatus development. *BioEssays* **28**, 1078-1086.
Wyngaarden, L. A., Delgado-Olguin, P., Su, I. H., Bruneau, B. G. and Hopyan, S. (2011). Ezh2 regulates anteroposterior axis specification and proximodistal axis elongation in the developing limb. *Development* **138**, 3759-3767.
Yueh, Y. G., Gardner, D. P. and Kappen, C. (1998). Evidence for regulation of cartilage differentiation by the homeobox gene Hoxc-8. *Proc. Natl. Acad. Sci. USA* **95**, 9956-9961.
Zeng, X., Chen, S. and Huang, H. (2011). Phosphorylation of EZH2 by CDK1 and CDK2: a possible regulatory mechanism of transmission of the H3K27me3 epigenetic mark through cell divisions. *Cell Cycle* **10**, 579-583.